Fibroblast-Populated Collagen Microsphere Assay of Cell Traction Force: Part 1. Continuum Model

Alice G. Moon and Robert T. Tranquillo
Dept. of Chemical Engineering and Materials Science, University of Minnesota, Minneapolis, MN 55455

The most popular in vitro assay currently used to characterize cell traction forces exerted on extracellular matrix (ECM) fibers is the fibroblast-populated collagen lattice (FPCL) assay. The compaction of a disk of cell-populated collagen gel, in terms of rate or extent of diameter reduction, is typically reported as the measure of cell traction. This measure, however, depends on assay properties incidental to the intrinsic traction, such as the initial cell concentration, the initial collagen concentration, and the geometry of the gel. Thus, there is a clear need to identify and measure an objective index of cell traction. Here, we propose as such an index a traction parameter (reflective of the cell-fiber mechanical interaction) defined in a continuum theory in which the interactive processes of cell motility and ECM deformation are modeled by expressions for cell and ECM conservation coupled to the mechanical force balance for the cell-ECM composite. The equations are formulated and solved for our adaptation of the FPCL assay in which cells are initially dispersed in a collagen gel microsphere, conferring several experimental and theoretical advantages over the popular disk geometry. The solution of the nonlinear system of partial differential equations (parameterized on the traction parameter) is then compared to compaction data for the fibroblast-populated collagen microspheres (FPCM). We show that the model predictions are consistent with the data when the initial cell concentration and the initial FPCM diameter are varied. In Part 2, we show how these results, along with the determination of the growth parameters of the cells and the viscoelastic parameters of the gel, have allowed us to estimate the magnitude of the traction parameter, which is a direct measure of the traction exerted by fibroblasts in a physiologically relevant collagen gel.

Introduction

The mechanical interaction of motile cells with fibers in the surrounding extracellular matrix (ECM), leading to reorganization and compaction of fibrillar protein networks, is fundamental to cell behavior in soft tissues and tissue-equivalent reconstituted collagen gels, and thus to many problems spanning biomedicine to biotechnology. Such cell-matrix interactions are manifest, for example, in wound healing, tissue regeneration, bioartificial skin and organ development and function, and mammalian cell immobilization in bioreactors (Montandon et al., 1977; Ehrlich, 1988; Yannas et al., 1982; Trinkaus, 1984; Madri and Pratt, 1986; Nilsson and Mosbach, 1987; Nilsson et al., 1983).

Correspondence concerning this article should be addressed to R. T. Tranquillo.

Harris and coworkers were the first to propose that the reorganization of fibrils around cells dispersed in a reconstituted type I collagen gel (Figure 1) is a direct consequence of cell traction forces, cytoplasmic forces transmitted by cell protrusions to the collagen fibrils (Harris et al., 1981). The dramatic, macroscopic manifestation of this phenomenon was documented earlier by Bell and coworkers who conducted a study based on their seminal fibroblast-populated collagen lattice (FPCL) assay (Bell et al., 1979). They exploited the ability to evaluate cell behavior in the physiologically relevant environment of a type I collagen gel, made by restoring a dilute aqueous solution of collagen to physiological conditions in order to initiate collagen fibrillogenesis (as popularized by Elsdale and Bard (1972)). They observed that fibroblasts in-

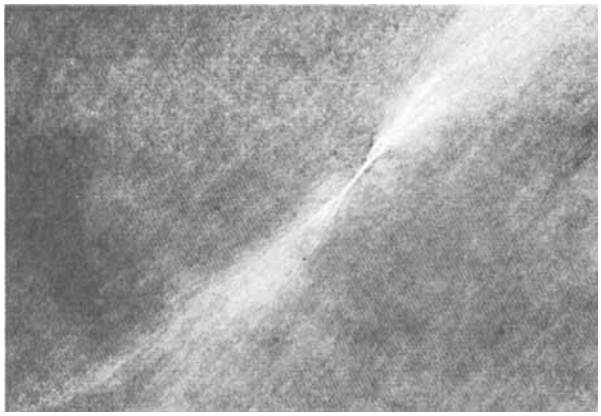

Figure 1. Cell traction forces manifested as restructuring of local collagen fibrils.

The polarized light micrograph shows bright regions extending outward from the pseudopods (extending and retracting cell processes) of a human foreskin fibroblast cultured in a reconstituted collagen gel, indicating that traction forces exerted by the cell on proximal collagen fibrils can cause restructuring of the local collagen network.

corporated in a small disk of collagen gel floating in culture media can compact the gel to a small fraction of its initial volume, displacing medium from the gel while organizing and concentrating the collagen fibrils—a cell-induced syneresis of the gel. Based on measurements of the disk diameter with time, it was determined that the rate and extent of gel compaction decreased as a function of the initial collagen concentration and increased as a function of the initial cell concentration over the ranges tested.

The FPCL assay and its variants quickly became established as the primary means of investigating the ability of normal (Bellows et al., 1981; Grinnell and Lamke, 1984; Ehrlich et al., 1986) and pathological cells (Buttle and Ehrlich, 1983; Delvoye et al., 1983) to mechanically interact with the ECM, including assessment of the effects of various pharmacological mediators (Leader et al., 1983; Danowski and Harris, 1988), serum factors (Gillery et al., 1986; Montesano and Orci, 1988) and other ECM components (Guidry and Grinnell, 1987) on type I collagen gel compaction. Grinnell and coworkers conducted a series of investigations to elucidate the mechanism of fibril organization and gel compaction (Grinnell and Lamke, 1984; Guidry and Grinnell, 1985, 1986, 1987). Several important observations and conclusions have been made: fibrils in the gel interior are rearranged even when the cells are only at the surface, and disrupting the network connectivity inhibits compaction, both implying the transmission of traction force through a connected fibrillar network of collagen; only 5% of the collagen is degraded in short-term culture even though the gel volume may decrease by 85% or more, implying compaction involves primarily a rearrangement of existing collagen fibrils rather than their degradation and replacement; few covalent modifications of the collagen occur; a partial reexpansion of compacted gels occurs after treatment of the cells with cytochalasin D or removal of the cells with detergent; and cell-free gels compacted under centrifugal force exhibit a partial reexpansion similar to the fibroblast-compacted gels. Based on these observations, a two-step mechanism was hypothesized for the mechanical stabilization of collagen fibrils during gel compaction: cells pull collagen fibrils into proximity via pseudopods exerting traction, and over a longer time scale, the fibrils become noncovalently crosslinked, independent of cell-secreted factors (Guidry and Grinnell, 1986).

Despite the significant understanding that has been obtained from the FPCL assay about cell-ECM mechanical interactions, there is a fundamental limitation in characterizing the compaction simply in terms of rate or extent of disk diameter reduction. Both of these measures are dependent on assay properties that complicate the interpretation of the traction being exerted by the cells, such as the initial cell concentration and the collagen concentration, or properties that are completely irrelevant, such as the geometry of the gel. The viscoelastic properties of the gel, for example, are highly dependent on the collagen concentration, so the measured compaction driven by cell traction is directly dependent on the collagen concentration. Consequently, the usual reported measures of compaction are not objective indices of cell traction, and are thus unsatisfactory from a scientific viewpoint. There is a clear need, then, to identify an objective index of traction that can be measured in the FPCL assay, another type of population assay, or a single cell assay. In addition to the usual statistical disadvantages of single cell measurements, the dimensions of a cell and the magnitude of its traction are far too small to be within the operating range of conventional mechanical testing devices, even if the normal cell-gel environment could be created and maintained. Therefore, it is necessary to develop a phenomenological theory or validate an existing one that includes all the necessary parameters to describe the state of stress in a cell-collagen gel continuum (particularly a traction parameter reflecting the intrinsic force transmitted through a cell-fibril mechanical interaction) and that can be used to model the relevant population assay. This theory would necessarily include aspects of cell dynamics (that is, mitosis, migration, and convection) as well as the mechanics of the cell-gel composite.

Here we formulate and summarize the analysis of a mathematical model for a spherical analogue of the traditional FPCL assay based on a monophasic continuum theory of cell-ECM mechanical interactions proposed by Murray and Oster (1984). The spherical geometry of a fibroblast-populated collagen microsphere (FPCM) has several key advantages. First, the spherically symmetric set of equations of the mathematical model are far simpler to solve than those applicable to the original disk geometry (that is, inherently one- rather than two-space dimensional). Second, the FPCM preparation protocol yields collagen fibril orientation that is relatively isotropic initially, consistent with the desirable simplifying assumptions outlined below and unlike the traditional FPCL assay, where fibrillogenesis in the presence of bounding surfaces can lead to significant local anisotropy (Modis, 1991). Third, the FPCM can be prepared at arbitrarily small diameters and still compact uniformly, which allows diffusion gradients of nutrients and metabolites to be minimized. This is not the case with the thin disk geometry of the FPCL assay. In addition, the FPCM assay of cell traction closely resembles our novel dermal wound contraction assay, wherein the microsphere center is initially devoid of cells but contains a diffusable mediator of fibroblast proliferation or migration, representing the initial inflammatory state of a full thickness wound (Tranquillo et al., 1992).

Such a wound assay configuration must be of spherical geometry to most conveniently and predictably establish concentration gradients of cellular mediators by diffusion, and this allows a desirable close correspondence between the two assays in terms of protocols, conditions, and measurement techniques. As will be seen, the advantages of the FPCM configuration come with only a very modest increase in experimental effort.

There are two significant benefits of a validated predictive model for the FPCM traction assay: the possibilities of measuring the objective traction parameter defined in the Murray and Oster theory, and extending the model to the related FPCM wound assay. Measuring the traction parameter entails having to independently validate the functionality and measure the parameters for all terms in the model equations other than the traction term of interest. This is quite feasible, as described in the second part of this work (Moon and Tranquillo, submitted).

Materials and Methods

Cell cultures

Human skin fibroblast cultures are first initiated from neonatal foreskins (see description of primary culture technique in Freshney, 1987). Cells are subsequently grown in 75 cm^2 tissue culture flasks containing Dulbecco's modified Eagle medium (DMEM) supplemented with 20% fetal bovine serum (FBS), penicillin/streptomycin, and Fungizone. Cultures are maintained at 37°C in a humidified incubator with an atmosphere of 10% CO_2–90% air. The fibroblasts are harvested prior to confluency with a 0.25% trypsin solution. Cultures are split four ways for passing and discarded prior to the tenth passage.

Collagen solution

Vitrogen 100 collagen (Celtrix Laboratories) is a sterile solution of 99.9% pure pepsin-digested bovine dermal collagen dissolved in 0.012 N HCl at a concentration of 3.0 mg/mL. It consists of 95–98% type I collagen (largely monomeric) with the remainder being type III collagen.

FPCM preparation

Cold Vitrogen 100 solution (730 μL) is adjusted to physiological ionic strength and pH (7.4) with the addition of 20 μL of 1 M HEPES buffer solution, 90 μL 10X Medium 199 (M199), 30 μL FBS, and 130 μL of 0.1 M NaOH. A small volume of a concentrated cell suspension in growth medium is added to yield the desired final cell concentration. The final collagen concentration is 2.1 mg/mL as standard. The cells are added after the solution pH is adjusted and suspended in the mixture immediately after the Vitrogen 100 is added to ensure the cells are entrapped during fibrillogenesis when the solution is heated to 37°C. After 3 minutes, about 0.5 μL of the partially gelled preparation is micropipetted into a test tube containing silicone fluid (Harwick SF 1250) at 37°C to yield an FPCM of around 1 mm diameter. After 7 additional minutes the FPCM is sufficiently gelled to allow isolation. The silicone fluid is drawn off and replaced by M199 with 20% FBS in a multiwell culture dish for microscopic observation.

FPCM diameter measurements

The FPCM diameters are measured using a Zeiss Axiovert 10 inverted light microscope in brightfield, a Hamamatsu C2400 Newvicon camera system, and a Kontron Electronics IBAS image analysis system. The FPCM are maintained under atmospheric conditions at 37°C with an air stream incubator. The microscope is focused to the image plane with the largest image area, representing the center cross-section of the FPCM. A digitizing pad and mouse are used to mark the endpoints of line segments defining the diameter of the FPCM displayed on the IBAS image monitor. Eight or more measurements are taken at different orientations for each FPCM, and the diameter is taken as the average of these values. The FPCM diameter is measured immediately after preparation and at prescribed time points.

Maximum cell diameter measurements

The maximum cell diameters of a set of ten fibroblasts in an FPCM are measured using the same system described above. An average of the ten cell diameters is recorded as a function of time. As the magnification is very low in each case (as is necessary for the monitoring of the FPCM diameters over time), leading to poor spatial resolution of the cell outline, these measurements give only a semiquantitative analysis of the progression of cell spreading within the FPCM with time.

Cell viability determination

The FPCM were stained with the fluorescent vital dyes fluorescein diacetate (FDA) and ethidium bromide (EB) to determine cell viability. The staining solution was prepared using 10 mL of EB stock solution (20 μg/mL in phosphate buffered saline (PBS)) and 10 μL of FDA stock solution (5 mg/mL in acetone). Medium was first drawn off each FPCM and enough FDA/EB solution was added to cover the sample. After four minutes the staining solution was removed and replaced with PBS. The FPCM were promptly examined with the inverted light microscope using epifluorescence. Only live cells are able to cleave the ester linkage in FDA, resulting in green cytoplasmic fluorescence. The polarized fluorescein molecule is unable to pass back across the intact cell membranes of live cells, causing accumulation of fluorescent fluorescein within the cell (Gray and Morris, 1987). EB rapidly penetrates membranes of dead cells, binding to nuclear DNA and emitting red fluorescence (membranes of live cells are penetrated only very slowly). Thus, live and dead cells are easily distinguished by green and red fluorescence, respectively, with this protocol.

Monophasic Theory of Cell-ECM Mechanical Interactions

The phenomenological theory developed by Oster, Murray, and coworkers (Murray et al., 1983; Oster et al., 1983; Murray and Oster, 1984) is a continuum theory that accounts for known cell behavioral properties, such as migration and mitosis, and the coupling of cell traction forces to the mechanical state of the ECM. This coupling leads to a predicted traction-induced deformation of the ECM. The Oster et al. theory is summarized below in their notation.

In its simplest form, there are three variables in the for-

mulation: the local cell concentration, $n(\underline{x}, t)$, the local ECM concentration, $\rho(\underline{x}, t)$, and the displacement vector for the cell/ECM composite, $\underline{u}(\underline{x}, t)$ ($\underline{u}$ is the vector connecting a material point in the composite located at position $\underline{x}$ at time t with its initial position, $\underline{x}_0$, that is, $\underline{x}_0(\underline{x}, t) + \underline{u}(\underline{x}, t) = \underline{x}$. It measures the magnitude and direction of displacement of a material point due to acting forces). These variables satisfy equations deriving from the fundamental laws of species conservation, yielding equations describing n and ρ, and linear momentum conservation, yielding the equation describing $\underline{u}$. The specific terms of these equations depend, of course, on both the phenomena presumed operative as well as how they are modeled.

The species conservation equations express the requirement that the rate of accumulation of a species in a control volume equals the net flux of the species through the boundaries of the control volume plus the net rate of generation within the control volume. For the cell conservation equation, this translates into a specification of terms reflecting net cell flux due to active migration, $\underline{J}_n$, and proliferation, R_n (Segel, 1980). In general form, the cell conservation equation describing the local cell concentration, $n(\underline{x}, t)$, is:

$$\frac{\partial n}{\partial t} + \nabla \cdot n \frac{\partial \underline{u}}{\partial t} = -\nabla \cdot \underline{J}_n + R_n \tag{1}$$

The convective term is a contribution to the net cell flux by virtue of convection of the ECM, in which the cells reside, with velocity $\partial \underline{u}/\partial t$ (that is, a time-dependent displacement).

The simplest case for specifying $\underline{J}_n$ is when the ECM environment is isotropic. In that case, a cellular analogy of Fick's law ($\underline{J}_n = -\mathcal{D}\nabla n$) is known to accurately model the resultant random migration (that is, persistent random walk) of blood and tissue cells in isotropic environments, assuming sufficiently low cell concentrations such that the cells move independently. This has been documented for embryonic fibroblasts migrating in a type I collagen gel (Noble and Shields, 1989). Modeling of biased migration is assumed unnecessary given the initial homogeneous, isotropic state of the collagen gel in our assay, but essentially amounts to additional terms in $\underline{J}_n$ (for example, Tranquillo and Lauffenburger, 1991; Dickinson and Tranquillo, 1993). Our choice for modeling the net rate of fibroblast proliferation is the logistic rate law, or cell concentration-regulated growth, which has been demonstrated for fibroblasts cultured in type I collagen gel (Schor, 1980). With these assumptions, Eq. 1 becomes:

$$\frac{\partial n}{\partial t} + \nabla \cdot n \frac{\partial \underline{u}}{\partial t} = \mathcal{D}\nabla^2 n + kn(N - n) \tag{2}$$

The cell random motility coefficient, $\mathcal{D}$, "growth" rate constant ("growth" here is meant to indicate cell division), k, and maximum concentration, N, are all assumed to be constant in our assay (N is determined by unknown cell regulatory mechanisms and depends on the extracellular environment as well as the cell type).

For the ECM conservation equation, terms reflecting transport and net synthesis of the ECM must be specified. In this monophasic theory, "ECM" means the fiber network and surrounding fluid considered together as a single, homogeneous phase (that is, a compressible solid), and in the ECM conservation equation, unlike the momentum conservation equation below, the presence of cells is essentially ignored. Since the ECM is assumed to be constituted of a fibrillar network, there is only a convective component to its flux (the network cannot diffuse). With these assumptions, the ECM conservation equation describing the local ECM concentration, $\rho(\underline{x}, t)$, in analogy to Eq. 1, is simply:

$$\frac{\partial \rho}{\partial t} + \nabla \cdot \rho \frac{\partial \underline{u}}{\partial t} = R_\rho \tag{3}$$

The equation of motion deriving from momentum conservation, which describes the local displacement of a material point of the cell/ECM composite, $\underline{u}(\underline{x}, t)$, is simplified given the fact that inertial forces are negligible for cell/ECM mechanics (Odell et al., 1981), yielding a mechanical force balance between cell traction and forces associated with the ECM physico-chemical properties. In its most general form, the mechanical force balance involves the total stress tensor for the cell/ECM composite, σ, and the net body force acting on a volume element of the composite, $\underline{f}$:

$$\nabla \cdot \sigma + \rho \underline{f} = \underline{0} \tag{4}$$

Oster, Murray, and coworkers assume that the traction exerted by cells resident within the ECM can be modeled as an active stress, so that σ can be written as the sum of the stress tensors describing the ECM alone, σ_{ECM}, and that associated with the traction stress, $\sigma_{\text{Cell/ECM}}$:

$$\nabla \cdot [\sigma_{\text{ECM}} + \sigma_{\text{Cell/ECM}}] + \rho \underline{f} = \underline{0} \tag{5}$$

At this stage, the treatment of momentum conservation is quite general. However, in order to proceed, constitutive forms for σ_{ECM} and $\sigma_{\text{Cell/ECM}}$ must be specified.

The simplest relevant form for σ_{ECM} is an isotropic, linear viscoelastic stress tensor. This assumption is only consistent with sufficiently small strains, such that material and geometrical nonlinearities as well as anisotropy associated with strain-induced fibril alignment are not significant. Following Oster, Murray, and coworkers, we use the following constitutive expression for the ECM (Landau and Lifshitz, 1970):

$$\sigma_{\text{ECM}} = \mu_1 \frac{\partial \epsilon}{\partial t} + \mu_2 \frac{\partial \theta}{\partial t} I + \left(\frac{E}{(1+\nu)}\right)\left[\epsilon + \left(\frac{\nu}{(1-2\nu)}\right)\theta I\right]$$

$$\epsilon = \frac{1}{2}(\nabla \underline{u} + \nabla \underline{u}^T) = \text{strain tensor}$$

$$\theta = \nabla \cdot \underline{u} = \text{dilation} \tag{6}$$

where μ_1 and μ_2 are related to the shear, μ, and bulk, K, viscosities ($\mu_1 = 2\mu$, $\mu_2 = K - 2/3\mu$), E is Young's modulus, and ν is Poisson's ratio.

The form proposed by Oster, Murray, and coworkers for $\sigma_{\text{Cell/ECM}}$, which we have also adopted, views cell traction as a "negative pressure" proportional to the product $n \cdot \rho$ (implying a rapid equilibrium of pseudopod-fiber anchorage interactions or receptor-mediated adhesions), where the proportionality

constant, τ, reflects the traction stress generated per unit cell and ECM concentrations. In order to accommodate the *in vitro* observation of contact inhibition of motility, and therefore presumably of traction, for cells in physical contact on planer substrata, Oster et al. assume τ to be a monotonic decreasing function of cell concentration: $\tau(n) = \tau_0(1 + \lambda n^2)^{-1}$, where τ_0 is the traction parameter [with units of dyne·cm^4/(mg collagen·cell)] and λ is a contact inhibition parameter. These assumptions lead to:

$$\sigma_{\text{Cell/ECM}} = \tau_0 \frac{\rho n}{1 + \lambda n^2} I \tag{7}$$

where I is the unit tensor. Thus, τ_0 is a measure of the traction exerted by a cell on local ECM fibers, reflecting the innate ability of the cell to generate motile force and the efficiency with which the cell transmits this force to fibrils via pseudopod-fiber interactions. Motile force here refers to actomyosin-based contractile force developed in the actin filament network which comprises pseudopods.

Equations 1, 3, and 5 comprise the most general starting form of the monophasic cell traction theory considered here, with the key term being the active traction stress, $\sigma_{\text{Cell/ECM}}$, which couples cell and ECM dynamics with deformation of the cell/ECM composite.

Experimental Results

The compaction behavior of the fibroblast-populated microspheres in our FPCM assay is qualitatively similar to that reported for the fibroblast-populated disks in the traditional FPCL assay (Figure 2). Initially, the cells are distributed uniformly throughout and exhibit a spherical morphology. The FPCM are also quite spherical before the onset of compaction, with less than 1% standard deviation in the initial diameter measurements. Over a period of about five to fifteen hours (depending on the initial cell concentration), the cells develop a characteristic stellate morphology. After this initial lag time for cell spreading, compaction proceeds and the gel gradually becomes opaque due to the exclusion of medium and tight packing of collagen fibrils by the cells. At 10% compaction (based on diameter reduction), the FPCM are only slightly less uniform, with typically 2.5% standard deviation in the diameter measurements. The viability is >95% across the FPCM over the time-course of the assay based on the FDA/EB cell viability assay, indicating that there is no toxic effect of the silicon fluid used in the preparation procedure and that adequate nutrient and metabolite transfer is taking place. No compaction is observed for control microspheres prepared with fibroblast-conditioned medium instead of cells.

A typical time-course of compaction is presented in Figure 3 for three different initial cell concentrations, n_0, with the same initial FPCM diameter, D_0. As previously reported for the FPCL assay (Bell et al., 1979), the rate and extent of gel compaction increases with increasing initial cell concentration in our FPCM assay (within the range tested). We have evidence that the lag time preceding the active phase of compaction may be explained, at least in part, by the initial period required for cells to spread from the rounded state observed when the FPCM is prepared to their stellate morphology (expression of motility and traction typically accompanies cell spreading). A

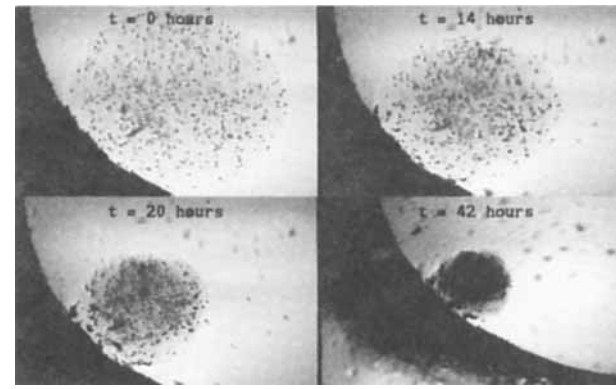

Figure 2. Fibroblast-populated collagen microsphere (FPCM) assay of cell traction.

The initial state of the FPCM (first panel) and several subsequent states during the time course of compaction (final three panels). Here, the fibroblasts are dispersed uniformly throughout the assay at an initial concentration of 3.5×10^5 cells/mL and the initial FPCM diameter is 1.3 mm.

comparison of the population average of maximum cell dimension and FPCM compaction over time is shown in Figure 4. The upward break in the maximum cell diameter curve corresponds to the initial spreading of cells and correlates with the initiation of compaction. These results support the strong correlation between the length of the lag time before initiation of gel compaction and the average time required for fibroblast elongation previously reported by Nishiyama and coworkers (Nishiyama et al., 1988). Note that only the initial part of the compaction curve is relevant for comparison to the model

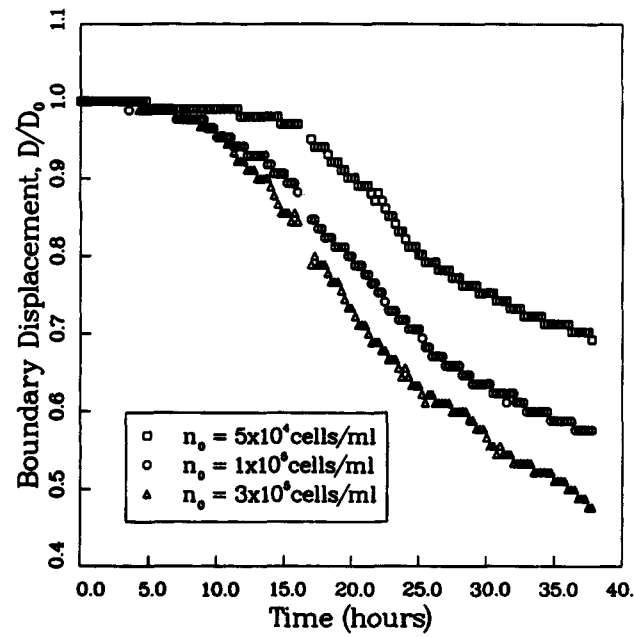

Figure 3. Observed dependence of compaction in the FPCM traction assay on initial cell concentration, n_0.

In each case, the initial FPCM diameter, D_0, is close to 0.9 mm.

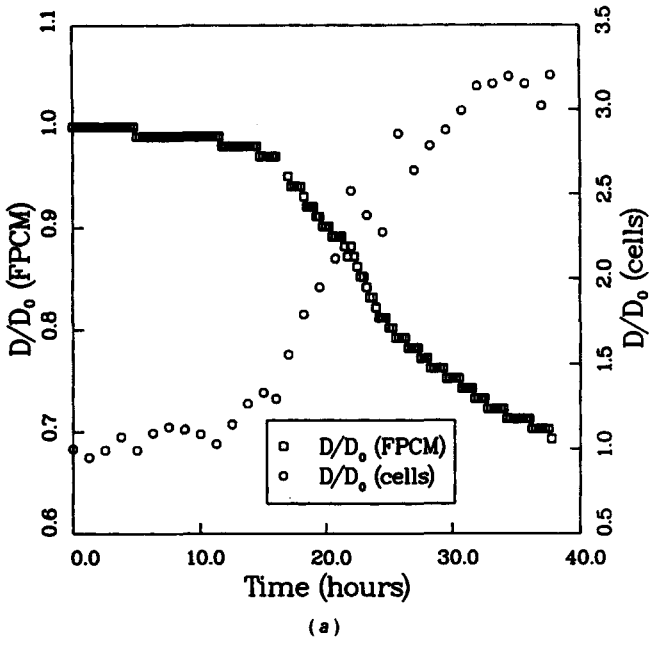

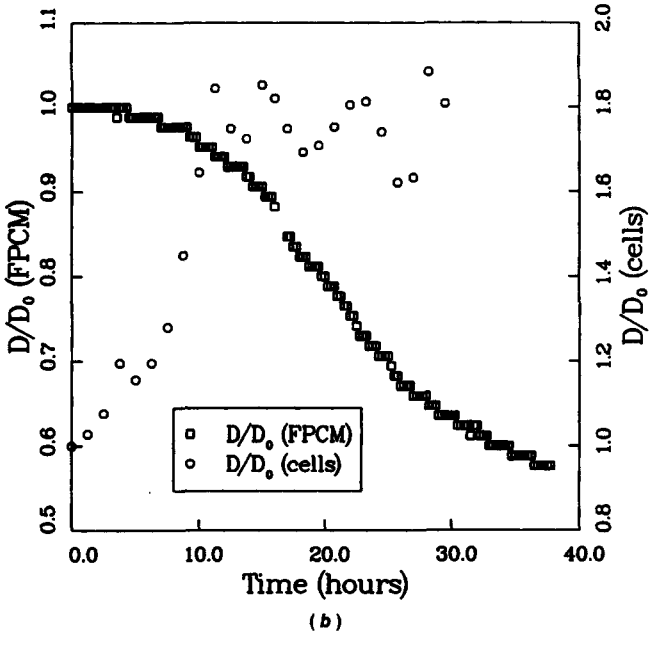

Figure 4. Comparison of the progression of cell spreading with gel compaction in the FPCM traction assay for initial cell concentrations of (a) $n_0 = 5.0 \times 10^4$ cells/mL and (b) $n_0 = 1.0 \times 10^5$ cells/mL.

The instantaneous diameters of the FPCM and the cells are scaled to their initial diameters, D_0.

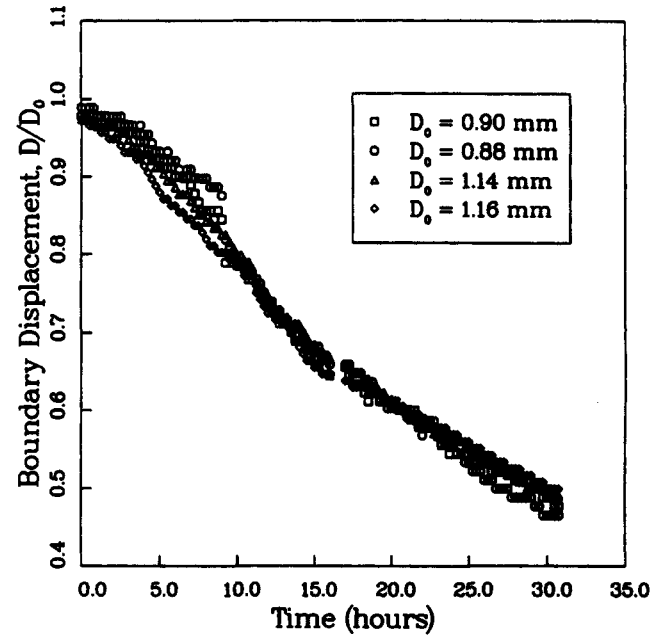

Figure 5. Observed dependence of compaction in the FPCM traction assay on initial microsphere diameter, D_0.

In each case, the initial cell concentration, n_0, is 3.0×10^5 cells/mL.

predictions given the small strain assumption implicit in Eq. 6.

The compaction curves in Figure 5 for duplicate trials at two different values of D_0, each with $n_0 = 3.0 \times 10^5$ cells/mL, are shifted along the time axis so that $t = 0$ corresponds to the beginning of the active phase of compaction. The rate and extent of compaction for all four FPCM in Figure 5 are approximately the same. The consistency between duplicates demonstrates excellent reproducibility. Although sphere diameter, as it determines surface area for syneresing medium, has been proposed to play a role in the chemically-induced syneresis of gels (Scherer, 1989), there appears to be a negligible effect over the range of diameters tested here (also indicating negligible gradients of nutrients and metabolites).

Mathematical Model: Formulation and Predictions

Our initial mathematical model for the FPCM assay is based on the monophasic theory of Oster et al. previously described. As noted earlier, the collagen fibril orientation is initially quite isotropic in the FPCM. Thus, we assume that Eqs. 2, 3, and 5-7 apply initially. In addition, we take $\underline{f} = \underline{0}$ (the free floating sphere experiences negligible body forces) and $R_\rho = 0$ [in accord with the observation that fibroblasts in a type I collagen gel do not extensively degrade the fibrils nor secrete significant amounts of new collagen that is incorporated into the network over the time scale of interest (Nusgens et al., 1984; Guidry and Grinnell, 1985)]. Because of the approximating spherical symmetry of the assay, only the radial component of $\underline{u}$, $u = u_r$, needs to be considered (that is, $u_\theta = u_\phi = 0$ by assumption).

It is necessary to prescribe initial and boundary conditions on the variables n, ρ, and u. From symmetry, we require the spatial derivative of n to be zero at the origin. We also assume that cells are confined within the FPCM. Combined with the previous assumption implicit in Eq. 2 that cells migrate only randomly, this requires that the spatial derivative of n be zero on the FPCM surface. These lead to the following boundary conditions on n:

$$\frac{\partial n}{\partial r}=0,\ r=0 \tag{8a}$$

$$\frac{\partial n}{\partial r}=0,\ r=S(t) \tag{8b}$$

where $S(t)$ denotes the position of the moving FPCM surface during compaction.

Again from symmetry, we require that there be no net displacement at the origin. We also assume a zero normal stress condition at the moving FPCM surface (that is, the kinematic boundary condition under the assumption of negligible surface tension at the interface between the FPCM and suspending medium). Using Eqs. 6 & 7, these lead to the following boundary conditions on u:

$$u=0,\ r=0 \tag{9a}$$

$$\sigma_{rr}=(\mu_1+\mu_2)\frac{\partial^2 u}{\partial r\partial t}+\frac{2\mu_2}{r}\frac{\partial u}{\partial t}+\frac{E(1-\nu)}{(1+\nu)(1-2\nu)}$$

$$\times\left[\frac{\partial u}{\partial r}+\frac{\nu}{1-\nu}\left(\frac{2u}{r}\right)\right]+\tau_0\frac{\rho n}{1+\lambda n^2}=0,\ r=S(t) \tag{9b}$$

Finally, symmetry requires the spatial derivative of ρ to be zero at the origin, leading to:

$$\frac{\partial \rho}{\partial r}=0,\ r=0 \tag{10}$$

We assume the cells are uniformly dispersed in the FPCM when prepared. The initial conditions are therefore:

$$n(r,\ t_0)=n_0 \tag{11a}$$

$$\rho(r,\ t_0)=\rho_0 \tag{11b}$$

$$u(r,\ t_0)=0 \tag{11c}$$

(where $0<r<D_0$ and $t=t_0$ is taken to be the time at which the cells spread in the collagen gel and compaction commences, as indicated in Figure 4). The full parabolic/elliptic system of three nonlinear partial differential equations for n, ρ, and u associated with the spherically-symmetric forms of Eqs. 2, 3, and 5-7 was reduced to a differential/algebraic system using finite differences and the method of lines. The position of the moving sphere boundary was fixed by a transformation to new space coordinates (Crank, 1984): $\xi=r/S(t)$. This transformation fixes the moving FPCM surface at $\xi=1$ for all time. The resulting initial value problem was solved using Differential/Algebraic System Solver (DASSL), a code developed for the numerical solution of implicit systems of differential/algebraic equations (Petzold, 1983). A complete statement of the transformed problem is found in Appendix A. (All parameters and variables are in dimensionless form hereafter, as defined in Appendix A, unless reported with units.)

Representative model predictions parameterized on the traction parameter, τ_0, are presented in Figure 6. The "boundary displacement" plotted vs. time in Figure 6 is equivalent to

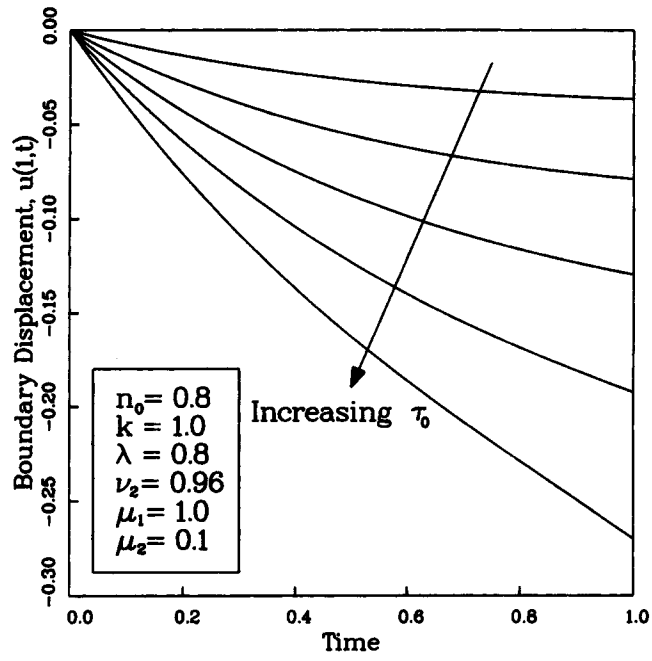

Figure 6. Prediction of compaction in the FPCM traction assay based on the monophasic theory, parameterized on the traction parameter, τ_0.

Model predictions are shown here for a dimensionless random motility coefficient, $\mathfrak{D}$, of both 0.001 and 1.0 (identical). τ_0 ranges from 0.2 to 1.0 (increments of 0.2).

$D(t)/D(0)-1$. Thus, neglecting the lag time due to cell spreading, Figures 3 and 6 are directly comparable. The values of the parameters were selected to give qualitative consistency with experimental data. The ultimate objective is to deduce the value of τ_0 from such a comparison when values for all the remaining parameters have been independently measured. The model predictions for the dependence of compaction on initial cell concentration, n_0, in Figure 7 are also qualitatively consistent with the data (Figure 3) at small values of τ_0 (that is, increasing rate and extent of compaction with increasing n_0). A crossover in the predictions is seen at large values of τ_0 due to the effect of contact inhibition at high cell concentrations. We have not observed this experimentally, indicating that contact inhibition of traction (if it occurs) is not significant in our assay at the cell concentrations tested.

Figure 8 presents predicted profiles for n, ρ and u at several times for the $\tau_0=1.0$ case of Figure 6. The radial displacement at the center of the sphere is zero, increasing linearly to a maximum displacement (negative displacement indicates compression) at the sphere surface (Figure 8a). The cell and ECM concentrations are both uniform in space and increase with time (Figures 8b and 8c). These results provide the basis for a more critical test of the model in conjunction with complementary measurements of tracer displacement and cell and collagen concentrations.

As is obvious from Figures 8a-8c, the system of three nonlinear partial differential equations can be shown to admit a solution of the form:

$$n(r,\ t)=n(t) \tag{12}$$

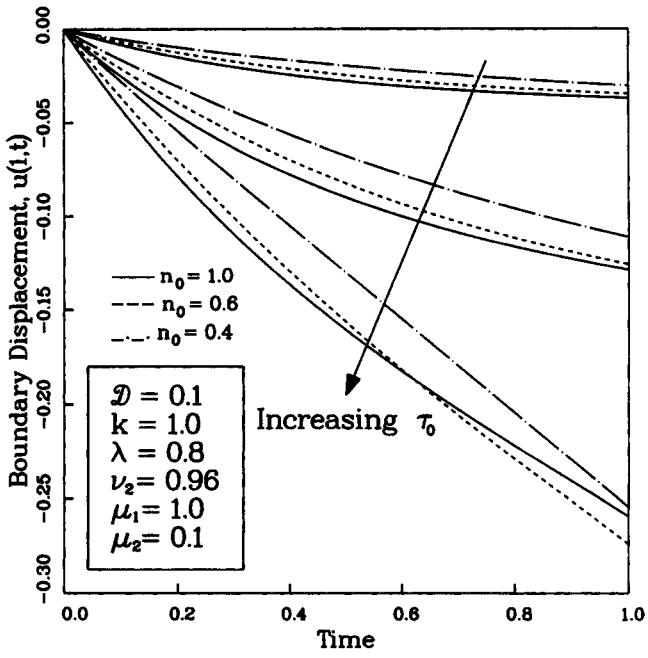

Figure 7. Dependence of model predictions of compaction in the FPCM traction assay on initial cell concentration, n_0.

τ_0 ranges from 0.2 to 1.0 (increments of 0.4).

$$\rho(r, t) = \rho(t) \tag{13}$$

$$u(r, t) = f(t) \cdot r \tag{14}$$

which satisfies the initial and boundary conditions, Eqs. 8-11 (Appendix B). Thus, one method for determining n, ρ, u, and $S(t)$ simply requires solving a set of five nonlinear coupled ordinary differential equations. In order to investigate the uniqueness of this solution, the initial cell profile was described as being randomly distributed around a uniform concentration (which has experimental relevance as well), and the full system of partial differential equations was solved numerically as described previously. With time, however, we observed an evolution to the "uniform" solution of Figure 8 for all cases studied (for example, Figure 9).

Discussion

We have presented results from an initial mathematical model for our FPCM assay of cell traction, a spherical analogue of the traditional FPCL assay. The spherical geometry was initially motivated by the desire to simplify analysis of the model equations, but it provides a number of significant advantages over the traditional disk geometry independent of the model, as we describe herein. The main goal of this work, however, is to measure a value for the traction parameter, τ_0, appearing in the Oster-Murray theory of cell-ECM mechanical interactions (which is the basis for our initial model) and, necessarily, test the validity of the theory for the fibroblast-populated collagen gel system. In this article, we show that the diameter reduction profiles with varied initial cell concentration and varied initial FPCM diameter are qualitatively consistent with the model predictions (Figures 3, 5, 6 and 7). In the second part of this article, we provide an initial estimate for τ_0 based on independent determination of the remaining model parameters (Moon and Tranquillo, submitted).

This work was motivated in part by the recognition that results for the FPCL assay as traditionally reported are not objective measures of cell traction. The model for our FPCM assay can be used to illustrate this point. In Figure 10a we predict the incubation time until some "target" level of compaction, t^*, here chosen as 10% reduction in diameter, as a function of the initial cell concentration, n_0, for a hypothetical set of parameter values. There are a range of n_0 values for which one might conclude that the same cell type exerts a different level of traction. For example, intuition might lead one to assume that doubling the initial cell concentration would decrease t^* by 50% (the "expected" curve). However, the model predicts that t^* is about 0.78 for $n_0 = 0.2$ and about 0.30 for $n_0 = 0.4$, or a decrease of 62%. Under the false assumption described above, which neglects the cell growth kinetics, one might conclude that the same cells exerted different traction in these two cases. A similar example can be given for drawing conclusions based on t^* for two cell types that really exert the same traction (that is, same τ_0) but have different growth kinetics, even when the same n_0 is used (Figure 10b). Other examples based on different values for the viscoelastic properties of the gel (associated with different initial collagen concentrations) that lead to false conclusions for the magnitude of cell traction could also be presented. These types of potential misinterpretations of the results from the FPCL and related assays serve to emphasize the need for the predictive modeling approach taken here.

Justification for many assumptions implicit in the elements of the Oster-Murray theory applied to the fibroblast-collagen gel system is provided herein. However, it is appropriate to provide a brief critique of the theory, with respect to validity for the FPCM assay, as motivation for continued investigation. First, it should be mentioned that the true form of the pivotal traction stress term of the theory, $\sigma_{\text{Cell/ECM}}$, remains an open question. While model predictions of the compaction profiles are qualitatively consistent with our preliminary data for the form employed, Eq. 7, critical evaluation is yet to be made for other predictions of the model (radial displacement, cell concentration, and collagen concentration profiles). In addition, independent, direct assessment of $\sigma_{\text{Cell/ECM}}$ should be obtained as a comparison to the model predictions. Two recent investigations of the isometric force generated in a slab of fibroblast-populated collagen gel (measured directly with a strain gauge type force transducer attached to one end of the slab) show some qualitative agreement with the results from both the traditional FPCM assay and the FPCM assay presented herein (Delvoye et al., 1991; Kolodney and Wysolmerski, 1992). For example, the steady-state force generated by the cells increased with increasing initial cell concentration at constant collagen concentration for the concentrations studied (Delvoye et al., 1991). Unfortunately, the slab of collagen gel is not elastic initially, and the measured forces are difficult to interpret directly until steady state, at which time the gel network has been highly compacted and may contain significant noncovalent crosslinks between fibrils (Guidry and Grinnell, 1986). Also, the slab becomes highly anisotropic by steady state, with fibrils and cells being coaligned with the strain

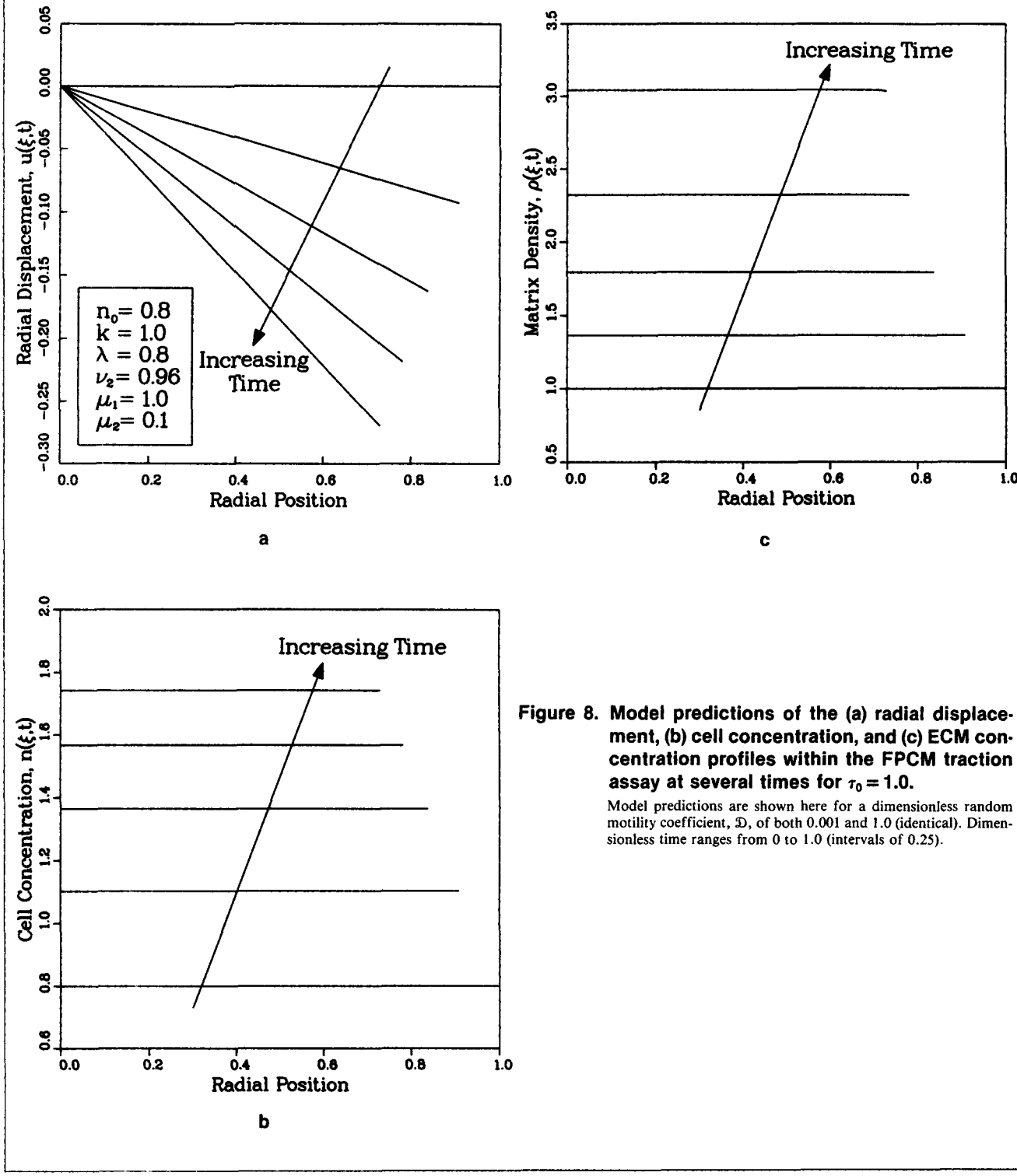

Figure 8. Model predictions of the (a) radial displacement, (b) cell concentration, and (c) ECM concentration profiles within the FPCM traction assay at several times for $\tau_0 = 1.0$.

Model predictions are shown here for a dimensionless random motility coefficient, $\mathfrak{D}$, of both 0.001 and 1.0 (identical). Dimensionless time ranges from 0 to 1.0 (intervals of 0.25).

gauge, inconsistent with the isotropic form currently assumed for $\sigma_{Cell/ECM}$ (valid only for initial compactions). Thus, although such experiments yield relevant data, direct determination of a valid functionality of $\sigma_{Cell/ECM}$ remains to be conducted.

A related issue involves the nature of the motility mechanism by which cells, fibroblasts in particular, mechanically interact with ECM fibers (Ehrlich et al., 1986; Ehrlich and Rajaratnam, 1990). Although a growing consensus supports the idea of "traction forces" associated with the continuous pseudopodal activity underlying locomotion of cultured fibroblasts (Harris et al., 1980, 1981, 1984; Harris, 1982, 1984), another view has proposed the forces to be "contraction forces" associated with the hypothesized shortening of the entire cell body characteristic of smooth muscle cell-like myofibroblasts (Gabbiani et

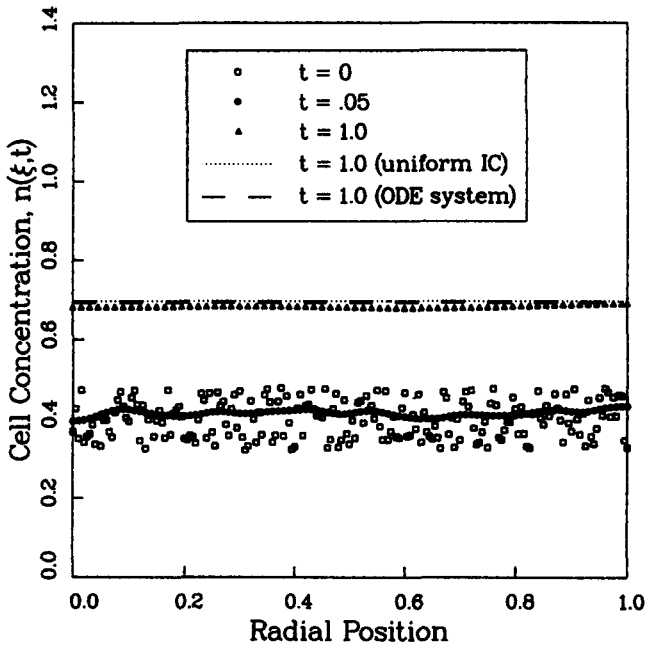

Figure 9. Predicted progression of a randomly distributed initial cell profile with time (symbols) and comparison to the profile for the uniform initial condition at $t = 1.0$ in the FPCM traction assay.

Also shown is the profile at $t = 1.0$ obtained from the reduced ODE system. $n_0 = 0.4$, $\mathfrak{D} = 0.01$, $k = 1.0$, $\lambda = 0.8$, $\nu_2 = 0.54$, $\mu_1 = 0.62$, $\mu_2 = 0.44$, and $\tau_0 = 0.2$.

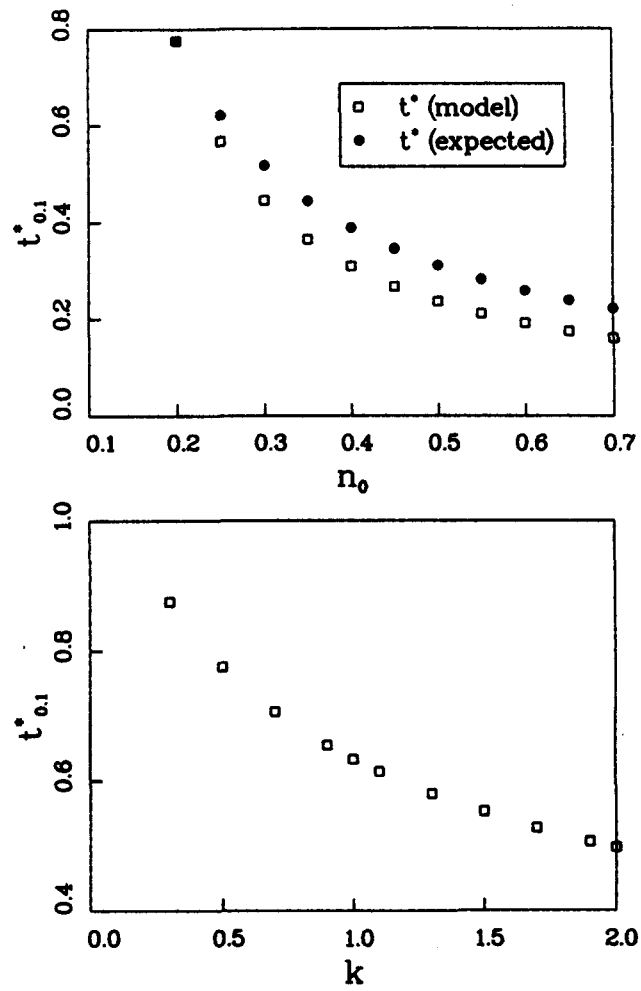

Figure 10. Predictions of the time required to reach 10% compaction in the FPCM traction assay ($t^*_{0.1}$) as a function of (a) initial cell concentration, n_0, (holding k constant at 0.5) and (b) dimensionless cell growth parameter, k (holding n_0 constant at 0.2).

$t^*_{0.1}$ (expected) = "expected" time to 10% compaction based on scaling $t^*_{0.1}$ obtained for $n_0 = 0.2$ by the value of interest $= 0.2 \cdot t^*_{0.1}/n_0$ (that is, if growth kinetics are ignored). In both cases, $\mathfrak{D} = 0.1$, $\lambda = 0.8$, $\nu_2 = 0.96$, $\mu_1 = 1.0$, $\mu_2 = 0.1$, and $\tau_0 = 1.0$.

al., 1971) (phenotypically modified fibroblasts observed in granulation tissue and in certain fibroses (Montandon et al., 1973; Guber and Rudolph, 1978; Skalli and Gabbiani, 1988) and also near the perimeter of the FPCL assay disk at high compaction (Nakagawa et al., 1989a,b; Ehrlich and Rajaratnam, 1990)). Fortunately, the modeling approach implicit in defining $\sigma_{\text{Cell/ECM}}$ is sufficiently abstract so as to accommodate both mechanisms. However, experiments conducted by Ehrlich et al. (1991) suggest that fibroblasts with pronounced cytoplasmic stress fibers and cell-cell attachments (characteristic of myofibroblasts), observed in the periphery of an FPCL assay disk, exert less force than fibroblasts with ordinary phenotype at the center, indicating a different τ_0 for a myofibroblast subpopulation. This would then require modeling the dynamics of the myofibroblast subpopulation with a species conservation equation like Eq. 2 extended to include a phenotype transformation term (see Tranquillo & Murray (1992) for a simpler approach when the transformation is governed by a paracrine growth factor).

Note that there is no explicit relationship between active migration and traction stress in the model (that is, the cell random motility coefficient, $\mathfrak{D}$, and the traction parameter, τ_0, are unrelated). However, motile but nontranslocating cells, as well as migrating cells, can be observed to locally restructure collagen fibrils *in vitro*, although it is not yet known whether they are exerting different magnitudes of traction. Thus, an explicit relationship between $\mathfrak{D}$ and τ_0 is perhaps unwarranted at this stage. In fact, the "uniform" solution we obtain for both the full PDE and reduced ODE (Appendix B) systems (Figure 9) does not depend on $\mathfrak{D}$. This is consistent with the uniform compaction predicted throughout the microsphere (that is, $u \propto r$) and the predicted uniform cell distribution, given the uniform initial state and the assumption of random migration. If a relationship between $\mathfrak{D}$ and τ_0 is warranted in the future, the isotropic form of $\sigma_{\text{Cell/ECM}}$ would be consistent only with this random migration case, as biased migration would be associated with net directional orientation of cells, that is, anisotropic traction stress. The possibility of oriented, motile but nontranslocating cells would also need to be considered, following from the discussion above.

Oster and Murray originally proposed their theory to investigate morphogenesis, where ECM referred to tissue. It has subsequently been applied to other *in vivo* processes involving

cell-tissue mechanical interactions, such as chondrogenesis (Oster et al., 1985) and wound contraction (Tranquillo and Murray, 1992). The idealization of ECM as a linear viscoelastic solid is better for tissue, where the fluid surrounding the fiber network is "ground substance" (a hydrophilic gel composed of glycosaminoglycans in tissue fluid and possessing electrostatic attraction for fixed charged proteoglycans bound to tissue fibers), than for our reconstituted collagen gel, where the fluid surrounding the (proteoglycan-free) collagen fibrils is low viscosity tissue culture medium. Invoking a monophasic postulate for intrinsically biphasic (fiber network plus fluid) materials creates several theoretical difficulties. First, the local concentration of ECM fibers is really the relevant quantity for ρ in $\sigma_{Cell/ECM}$ (Eq. 7), not ρ as defined (ECM fiber network plus fluid as a single phase). A more severe constraint of the monophasic model is that it is incapable of accounting for the cell-induced gel syneresis in our FPCM. Theoretically, this is manifested as an ill-defined Poisson's ratio for the gel. On a very short time scale (instantaneously applied stress), the gel is essentially incompressible ($\nu = 0.5$) since the solution cannot rapidly flow through the network. On a longer time scale (sustained stress), such as that relevant for the FPCM assay, the gel appears compressible ($0 < \nu < 0.5$) due to flow and loss of fluid (that is, due to the inherent biphasic nature), although ν would vary in some complex way as syneresis proceeds. Thus, although a degree of simplicity may be lost (as the "uniform" solution to the monophasic theory-based model equations for our FPCM assay requires only the numerical integration of five ordinary differential equations (Appendix B)), there is clear motivation to extend the current theory to account for the significant syneresis effect.

A model that describes fluid flow through a fibrillar network must make explicit account for conservation of mass and momentum for both the network and fluid phases, not a single "fluid/network ECM" phase as in the monophasic theory. We have recently developed one possible form of a biphasic theory that would be relevant for tissues and tissue-equivalent collagen gels that are populated by traction-exerting cells (Tranquillo et al., 1993). While it shares similarities with the monophasic theory presented here, such as an active stress term dependent on cell and network (not "ECM") concentrations, it also includes the frictional drag due to the relative velocities between flowing solution and displacing network, which is known to play an essential role in the apparent viscoelastic behavior of cartilage (Mak, 1986).

Finally, there is the unresolved issue of the initial lag period observed in the FPCM compaction curves. We have presented evidence (Figure 4) that this may be due, at least in part, to the initial time required for cell spreading. The observation that the lag has different duration depending on n_0 (Figure 3) suggests that there may be different accumulation rates of autocrine growth factors which stimulate cell spreading. However, a similar lag period has been observed for chemically-induced syneresing viscoelastic gels in which the crosslink density is increasing with time (Scherer, 1989). In order to resolve this issue, then, it will be necessary to ascertain whether such a crosslinking mechanism (as proposed by Guidry and Grinnell, 1986) is present and significant in the FPCM assay.

Although certain refinements can be made to current theory, the results presented herein, along with independently determined values of the cell and collagen gel model parameters appearing in the monophasic theory (excluding the cell traction parameter of interest, τ_0), provide the foundation for the first objective estimation of the traction forces exerted by fibroblasts cultured in a compacting collagen gel (Part 2 of this work). The measured values of τ_0 can then be legitimately compared for various cell types in a standard protocol, and the effect of cell stimuli (for example, growth factors) on τ_0 for a single cell type can also be investigated. There is recent evidence that stress or strain in an FPCM environment, both externally applied (Jain et al., 1990) and internally-induced by cell traction (Mochitate et al., 1991), can modulate cell metabolism and mitosis. Thus, in addition to providing a theoretical framework for objectively quantifying compaction in our FPCM traction and related FPCM wound assays (Tranquillo et al., 1993), this research should ultimately provide the rationale for identifying which properties of cell behavior or ECM must be altered in order to direct the reorganization of ECM fibers and thus optimize cell-ECM mechanical interactions in wound healing and other relevant biomedical and biotechnological processes.

Acknowledgment

This work has been supported by a National Science Foundation Presidential Young Investigator Award to Robert T. Tranquillo (NSF BCS-8957736). Initial support from an NIH Biomedical Research Support Grant administered by The Graduate School and a grant from the Minnesota Supercomputer Institute are acknowledged. Laboratory facilities provided by Dr. David Knighton, Department of Surgery, and technical advice of Vance Fiegal are also gratefully acknowledged, as are useful suggestions by the reviewers.

Notation

$a(t)$ = time-dependent function describing the linear dependence of $v(\xi, t)$ on ξ
D = sphere diameter
D_0 = initial sphere diameter
$\mathfrak{D}$ = cell random motility coefficient
E = Young's modulus
$f(t)$ = time-dependent function describing the linear dependence of $u(r, t)$ on r
$\underline{f}$ = body force
$h(t)$ = time-dependent function describing the linear dependence of $u(\xi, t)$ on ξ
I = unit tensor
$\underline{J}_n$ = net cell flux due to active migration
k = logistic growth rate constant
K = bulk viscosity
n = local cell concentration
n_0 = initial cell concentration
N = maximum cell concentration
r = radial coordinate
R_0 = initial sphere radius
R_n = net cell generation rate
R_ρ = net matrix generation rate
$S(t)$ = radial position of sphere boundary
t = time
t_0 = time zero
$t^*_{0.1}$ = time required for 10% compaction in FPCM assay
T = time scaling $= (\mu_1 + \mu_2)/E$
$\underline{u}$ = displacement vector for cell/matrix composite
u = radial displacement for cell/matrix composite
u_b = displacement at sphere boundary
u_r, u_θ, u_ϕ = spherical components of ECM displacement
v = radial velocity of cell/ECM composite
$\underline{x}$ = position vector
$\underline{x}_0$ = initial position vector

Greek letters

ϵ = infinitesimal strain tensor for cell/matrix composite
λ = contact inhibition parameter
μ = shear viscosity
$\mu_1 = 2\mu$
$\mu_2 = K - 2/3\mu$
$\theta = \nabla \cdot \underline{u}$, dilation of cell/ECM composite
ρ = local ECM concentration
ρ_0 = initial ECM concentration
σ = total stress tensor for cell/ECM composite
σ_{ECM} = stress tensor for ECM
$\sigma_{Cell/ECM}$ = stress tensor associated with the active traction stress
σ_{rr} = component of stress tensor normal to sphere boundary
τ = traction stress generated per unit cell and ECM concentrations
τ_0 = traction parameter
ν = Poisson's ratio
$\nu_1 = (1+\nu)(1-2\nu)/(1-\nu)$
$\nu_2 = \nu/(1-\nu)$
ξ = dimensionless radial coordinate in the transformed space

Superscript

* = indicates dimensionless quantity

Literature Cited

Bell, E., B. Ivarsson, and C. Merrill, "Production of a Tissue-like Structure by Contraction of Collagen Lattices by Human Fibroblasts of Different Proliferative Potential in vitro," *Proc. Nat. Acad. Sci. USA*, **76**, 1274 (1979).

Bellows, C. G., A. H. Melcher, and J. E. Aubin, "Contraction and Organization of Collagen Gels by Cells Cultured from Periodontal Ligament, Gingiva and Bone Suggest Functional Differences between Cell Types," *J. Cell. Sci.*, **50**, 299 (1981).

Buttle, D. J., and H. P. Ehrlich, "Comparative Studies of Collagen Lattice Contraction Utilizing a Normal and a Transformed Cell Line," *J. Cell Physiol.*, **116**(2), 159 (1983).

Crank, J., *Free and Moving Boundary Problems*, Oxford University Press, New York (1984).

Danowski, B. A., and A. K. Harris, "Changes in Fibroblast Contractility, Morphology, and Adhesion in Response to a Phorbol Ester Tumor Promoter," *Exp. Cell. Res.*, **177**(1), 47 (1988).

Delvoye, P., B. Nusgens, and C. M. Lapiere, "The Capacity of Retracting a Collagen Matrix is Lost by Dermatosparactic Skin Fibroblasts," *J. Invest. Dermatol.*, **81**(3), 267 (1983).

Delvoye, P., P. Wiliquet, J. L. Leveque, B. Nusgens, and C. Lapiere, "Measurement of Mechanical Forces Generated by Skin Fibroblasts Embedded in a Three-Dimensional Collagen Gel," *J. Invest. Dermatol.*, **97**, 898 (1991).

Dickinson, R. B., and R. T. Tranquillo, "A Stochastic Model for Cell Random Motility and Haptotaxis," *J. Math. Biol.*, in press (1993).

Ehrlich, H. P., "The Role of Connective Tissue Matrix in Wound Healing," *Prog. Clin. Biol. Res.*, **266**, 243 (1988).

Ehrlich, H. P., T. R. Griswold, and J. B. Rajaratnam, "Studies on Vascular Smooth Muscle Cells and Dermal Fibroblasts in Collagen Matrices. Effects of Heparin," *Exp. Cell Res.*, **164**(1), 154 (1986).

Ehrlich, H. P., and J. B. Rajaratnam, "Cell Locomotion Forces Versus Cell Contraction Forces for Collagen Lattice Contraction: an *in vitro* Model of Wound Contraction," *Tissue Cell*, **22**(4), 407 (1990).

Elsdale, T., and J. Bard, "Collagen Substrata for Studies on Cell Behavior," *J. Cell Biol.*, **54**, 626 (1972).

Freshney, R. I., *Culture of Animal Cells: A Manual of Basic Technique* (2nd Edition), Alan R. Liss, Inc., New York (1987).

Gabbiani, G., G. B. Ryan, and G. Majno, "Presence of Modified Fibroblasts in Granulation Tissue and their Possible Role in Wound Contraction," *Experientia*, **27**, 549 (1971).

Gillery, P., F. X. Maquart, and J. P. Borel, "Fibronectin Dependence of the Contraction of Collagen Lattices by Human Skin Fibroblasts," *Exp. Cell Res.*, **167**(1), 29 (1986).

Gray, D. W. R., and P. J. Morris, "The Use of Fluorescein Diacetate and Ethidium Bromide as a Viability Stain for Isolated Islets of Langerhans," *Stain Technol.*, **62**(6), 373 (1987).

Grinnell, F., and C. R. Lamke, "Reorganization of Hydrated Collagen Lattices by Human Skin Fibroblasts," *J. Cell Sci.*, **66**, 51 (1984).

Guber, S., and R. Rudolph, "The Myofibroblast," *Surg. Gynecol. & Obstet.*, **146**, 641 (1978).

Guidry, C., and F. Grinnell, "Studies on the Mechanism of Hydrated Collagen Gel Reorganization by Human Skin Fibroblasts," *J. Cell Sci.*, **79**, 67 (1985).

Guidry, C., and F. Grinnell, "Contraction of Hydrated Collagen Gels by Fibroblasts: Evidence for Two Mechanisms by which Collagen Fibrils are Stabilized," *Collagen Rel. Res.*, **6**, 515 (1986).

Guidry, C., and F. Grinnell, "Heparin Modulates the Organization of Hydrated Collagen Gels and Inhibits Gel Contraction by Fibroblasts," *J. Cell Biol.*, **104**(4), 1097 (1987).

Harris, A. K., "Traction and its Relations to Contraction in Tissue Cell Locomotion," *Cell Behaviour*, p. 77, R. Bellairs, A. Curtis and G. Dunn, eds., Cambridge University Press, New York (1982).

Harris, A. K., "Tissue Culture Cells on Deformable Substrata: Biomechanical Implications," *J. Biomech. Eng.*, **106**, 19 (1984).

Harris, A. K., D. Stopak, and P. Warner, "Generation of Spatially Periodic Patterns by a Mechanical Instability: a Mechanical Alternative to the Turing Model," *J. Embryol. Exp. Morphol.*, **80**, 1 (1984).

Harris, A. K., D. Stopak, and P. Wild, "Fibroblast Traction as a Mechanism for Collagen Morphogenesis," *Nat.*, **290**(5803), 249 (1981).

Harris, A. K., P. Wild, and D. Stopak, "Silicone Rubber Substrata: a New Wrinkle in the Study of Cell Locomotion," *Sci.*, **208**(4440), 177 (1980).

Jain, M. K., R. A. Berg, and G. P. Tandon, "Mechanical Stress and Cellular Metabolism in Living Soft Tissue Composites," *Biomat.*, **11**(7), 465 (1990).

Kolodney, M. S., and R. B. Wysolmerski, "Isometric Contraction by Fibroblasts and Endothelial Cells in Tissue Culture: a Quantitative Study," *J. Cell Biol.*, **117**, 73 (1992).

Landau, L. D., and E. M. Lifshitz, *Theory of Elasticity*, Pergamon Press, New York (1970).

Leader, W. M., D. Stopak, and A. K. Harris, "Increased Contractile Strength and Tightened Adhesions to the Substratum Result from Reverse Transformation of CHO Cells by Dibutyryl Cyclic Adenosine Monophosphate," *J. Cell Sci.*, **64**, 1 (1983).

Madri, J. A., and B. M. Pratt, "Endothelial Cell-Matrix Interactions: *in vitro* Models of Angiogenesis," *J. Histochem. Cytochem.*, **34**(1), 85 (1986).

Mak, A. F., "The Apparent Viscoelastic Behavior of Articular Cartilage—the Contributions from the Intrinsic Matrix Viscoelasticity and Interstitial Fluid Flows," *J. Biomech. Eng.*, **108**, 123 (1986).

Mochitate, K., P. Pawelek, and F. Grinnell, "Stress Relaxation of Contracted Collagen Gels: Disruption of Actin Filament Bundles, Release of Cell Surface Fibronectin, and Down-Regulation of DNA and Protein Synthesis," *Exp. Cell Res.*, **193**, 198 (1991).

Modis, L., *Organization of the Extracellular Matrix: A Polarization Microscopic Approach*, CRC Press, Boca Raton (1991).

Montandon, D., G. D'andiran, and G. Gabbiani, "The Mechanism of Wound Contraction and Epithelialization," *Clin. Plast. Surg.*, **4**(3), 325 (1977).

Montandon, D., G. Gabbiani, G. B. Ryan, and G. Majno, "The Contractile Fibroblast: Its Relevance in Plastic Surgery," *Plast. & Reconstr. Surg.*, **52**, 286 (1973).

Montesano, R., and L. Orci, "Transforming Growth Factor-β Stimulates Collagen-Matrix Contraction by Fibroblasts: Implications for Wound Healing," *Proc. Nat. Acad. Sci. USA*, **85**, 4894 (1988).

Moon, A. G., and R. T. Tranquillo, "The Fibroblast-Populated Collagen Microsphere Assay of Cell Traction Force: 2. Measurement of the Cell Traction Parameter," submitted (1992).

Murray, J. D., and G. F. Oster, "Cell Traction Models for Generating Pattern and Form in Morphogenesis," *J. Math. Biol.*, **19**(3), 265 (1984).

Murray, J. D., G. F. Oster, and A. K. Harris, "A Mechanical Model for Mesenchymal Morphogenesis," *J. Math. Biol.*, **17**(1), 125 (1983).

Nakagawa, S., P. Pawelek, and F. Grinnell, "Extracellular Matrix Organization Modulates Fibroblast Growth and Growth Factor Responsiveness," *Exp. Cell Res.*, **182**(2), 572 (1989a).

Nakagawa, S., P. Pawelek, and F. Grinnell, "Long-Term Culture of

Fibroblasts in Contracted Collagen Gels: Effects on Cell Growth and Biosynthetic Activity," *J. Invest. Dermatol.*, **93**(6), 792 (1989b).
Nilsson, K., and K. Mosbach, "Immobilized Animal Cells," *Dev. Biol. Standard*, **66**, 183 (1987).
Nilsson, K., W. Scheirer, O. W. Merten, L. Ostberg, E. Liehl, H. W. D. Katinger, "Entrapment of Animal Cells for Production of Monoclonal Antibodies and Other Biomolecules," *Nat.*, **302**, 629 (1983).
Nishiyama, T., N. Tominaga, K. Nakajima, and T. Hayashi, "Quantitative Evaluation of the Factors Affecting the Process of Fibroblast-Mediated Collagen Gel Contraction by Separating the Process into Three Phases," *Collagen Rel. Res.*, **8**, 259 (1988).
Noble, P. B., and E. D. Shields, "Time-Based Changes in Fibroblast Three-Dimensional Locomotory Characteristics and Phenotypes," *Exp. Cell Biol.*, **57**(5), 238 (1989).
Nusgens, B., C. Merrill, C. Lapiere, and E. Bell, "Collagen Biosynthesis by Cells in a Tissue Equivalent Matrix in vitro," *Collagen Relat. Res.*, **4**(5), 351 (1984).
Odell, G. M., G. Oster, P. Alberch, and B. Burnside, "The Mechanical Basis of Morphogenesis. I. Epithelial Folding and Invagination," *Dev. Biol.*, **85**(2), 446 (1981).
Oster, G. F., J. D. Murray, and A. K. Harris, "Mechanical Aspects of Mesenchymal Morphogenesis," *J. Embryol. Exp. Morphol.*, **78**, 83 (1983).
Oster, G. F., J. D. Murray, and P. K. Maini, "A Model for Chondrogenic Condensations in the Developing Limb: the Role of Extracellular Matrix and Cell Tractions," *J. Embryol. Exp. Morphol.*, **89**, 93 (1985).
Petzold, L. R., "A Description of DASSL: a Differential/Algebraic System Solver," *Scientific Computing: Applications of Mathematics and Computing to the Physical Sciences*, p. 65, R. S. Stepleman, ed., North-Holland Publishing Company, Amsterdam (1983).
Scherer, G. W., "Mechanics of Syneresis: I. Theory," *J. Non-Cryst. Solids*, **108**, 18 (1989).
Schor, S. L., "Cell Proliferation and Migration on Collagen Substrata in vitro," *J. Cell Sci.*, **41**, 159 (1980).
Segel, L. A., *Mathematical Models in Molecular and Cellular Biology*, Cambridge University Press, New York (1980).
Skalli, O., and G. Gabbiani, "The Biology of the Myofibroblast Relationship to Wound Contraction and Fibrocontractive Diseases," *The Molecular and Cellular Biology of Wound Repair*, p. 373, R. A. F. Clark and P. M. Henson, eds., Plenum Press, New York (1988).
Tranquillo, R. T., M. A. Durrani, and A. G. Moon, "Tissue Engineering Science: Consequences of Cell Traction Force," *Cytotechnology*, in press (1993).
Tranquillo, R. T., and D. A. Lauffenburger, "The Definition and Measurement of Cell Migration Coefficients," *Lect. Notes Biomath.*, **89**, 475 (1991).
Tranquillo, R. T., and J. D. Murray, "Continuum Model of Fibroblast-Driven Wound Contraction: Inflammation-Mediation," *J. Theor. Biol.*, **158**, 135 (1992).
Trinkaus, J., *Cells into Organs*, Prentice-Hall, Englewood Cliffs, NJ (1984).
Yannas, I. V., J. F. Burke, D. P. Orgill, and E. M. Skrabut, "Wound Tissue can Utilize a Polymeric Template to Synthesize a Functional Extension of Skin," *Sci.*, **215**(4529), 174 (1982).

Appendix A

The spherically-symmetric form of the equations for n, r, and u (Eqs. 2, 3, and 5-7) can be expressed in radial coordinates and in dimensionless form as:

Cell Conservation Equation:

$$\frac{\partial n}{\partial t}+\frac{\partial\left(n\,\frac{\partial u}{\partial t}\right)}{\partial r}+\frac{2n}{r}\frac{\partial u}{\partial t}=\mathfrak{D}\frac{\partial^2 n}{\partial r^2}+\frac{2\mathfrak{D}}{r}\frac{\partial n}{\partial r}+kn(1-n) \tag{A1}$$

Matrix Conservation Equation:

$$\frac{\partial \rho}{\partial t}+\frac{\partial\left(\rho\,\frac{\partial u}{\partial t}\right)}{\partial r}+\frac{2\rho}{r}\frac{\partial u}{\partial t}=0 \tag{A2}$$

Mechanical Force Balance:

$$\mu_1\frac{\partial}{\partial t}\left(\frac{\partial^2 u}{\partial r^2}+\frac{2}{r}\frac{\partial u}{\partial r}-\frac{2u}{r^2}\right)+\frac{\partial^2 u}{\partial r^2}+\frac{2}{r}\frac{\partial u}{\partial r}-\frac{2u}{r^2}+\frac{\partial\left(\frac{\tau_0 n\rho}{1+\lambda n^2}\right)}{\partial r}=0 \tag{A3}$$

The zero stress condition at the moving sphere boundary, Eq. 9b, can now be written as:

$$\frac{\partial u}{\partial r}+\nu_2\frac{2u}{r}+\mu_1\frac{\partial^2 u}{\partial r\partial t}+\frac{2\mu_2}{r}\frac{\partial u}{\partial t}+\tau_0\frac{\rho n}{1+\lambda n^2}=0,\quad r=S(t) \tag{A4}$$

where the dimensionless variables and parameters are:

$$n^*=\frac{n}{N}\quad \rho^*=\frac{\rho}{\rho_0}\quad u^*=\frac{u}{R}\quad r^*=\frac{r}{R}\quad t^*=\frac{t}{T}\quad \mathfrak{D}^*=\frac{\mathfrak{D}T}{R^2}$$

$$k^*=kNT\quad \lambda^*=\lambda N^2$$

$$\mu_1^*=\frac{\mu_1+\mu_2}{\mathrm{ET}}\nu_1\quad \mu_2^*=\frac{\mu_2\nu_1}{ET}\quad \tau_0^*=\tau_0\frac{\rho_0 N}{E}\nu_1$$

In these dimensionless groups, T is a characteristic time, chosen here to be the ECM viscous relaxation time, $(\mu_1+\mu_2)/E$, and

$$\nu_1=\frac{(1+\nu)(1-2\nu)}{(1-\nu)}\quad \nu_2=\frac{\nu}{1-\nu}$$

(The asterisks were suppressed in Eqs. A1-A4 and will be in all future dimensionless expressions for the sake of clarity.)

The moving sphere boundary in the problem outlined above can be fixed by a transformation to new space coordinates (Crank, 1984):

$$\xi=\frac{r}{S(t)} \tag{A5}$$

This transformation fixes the boundary at $\xi=1$ for all time. In order to transform the system of Eqs. A1-A3 from (r, t) space to (ξ, t) space, the following general relationships must be applied:

$$\frac{\partial u}{\partial r}=\frac{1}{S(t)}\frac{\partial u}{\partial \xi} \tag{A6a}$$

$$\frac{\partial^2 u}{\partial r^2}=\frac{1}{[S(t)]^2}\frac{\partial^2 u}{\partial \xi^2} \tag{A6b}$$

$$\left.\frac{\partial u}{\partial t}\right|_r=\frac{\partial u}{\partial \xi}\frac{\partial \xi}{\partial t}+\left(\frac{\partial u}{\partial t}\right)_\xi=-\frac{\xi}{S(t)}\frac{dS}{dt}\frac{\partial u}{\partial \xi}+\left(\frac{\partial u}{\partial t}\right)_\xi \tag{A6c}$$

Using these transformed derivative expressions (and similar expressions for ρ and n), and defining the cell/matrix composite velocity as:

$$v=\left(\frac{\partial u}{\partial t}\right)_{\xi} \tag{A7}$$

then the system of equations for the compacting microsphere problem can be written (for $0<\xi<1$ and $t>0$) as:

Cell Conservation Equation:

$$-\frac{\xi}{S}\frac{dS}{dt}\frac{\partial n}{\partial \xi}+\left(\frac{\partial n}{\partial t}\right)_{\xi}+\frac{n}{S}\frac{\partial}{\partial \xi}\left(-\frac{\xi}{S}\frac{dS}{dt}\frac{\partial u}{\partial \xi}+v\right)+\frac{1}{S}\left(\frac{\partial n}{\partial \xi}+\frac{2n}{\xi}\right)\left(-\frac{\xi}{S}\frac{dS}{dt}\frac{\partial u}{\partial \xi}+v\right)-\mathfrak{D}\left(\frac{1}{S^2}\frac{\partial^2 n}{\partial \xi^2}+\frac{2}{S^2\xi}\frac{\partial n}{\partial \xi}\right)+kn(n-1)=0 \tag{A8}$$

Matrix Conservation Equation:

$$-\frac{\xi}{S}\frac{dS}{dt}\frac{\partial \rho}{\partial \xi}+\left(\frac{\partial \rho}{\partial t}\right)_{\xi}+\frac{\rho}{S}\frac{\partial}{\partial \xi}\left(-\frac{\xi}{S}\frac{dS}{dt}\frac{\partial u}{\partial \xi}+v\right)+\frac{1}{S}\left(\frac{\partial \rho}{\partial \xi}+\frac{2\rho}{\xi}\right)\left(-\frac{\xi}{S}\frac{dS}{dt}\frac{\partial u}{\partial \xi}+v\right)=0 \tag{A9}$$

Mechanical Force Balance:

$$\frac{\partial^2 u}{\partial \xi^2}+\frac{2}{\xi}\frac{\partial u}{\partial \xi}-\frac{2u}{\xi^2}+\mu_1\frac{\partial^2}{\partial \xi^2}\left(-\frac{\xi}{S}\frac{dS}{dt}\frac{\partial u}{\partial \xi}+v\right)+\frac{2\mu_1}{\xi}\frac{\partial}{\partial \xi}\left(-\frac{\xi}{S}\frac{dS}{dt}\frac{\partial u}{\partial \xi}+v\right)-\frac{2\mu_1}{\xi^2}\left(-\frac{\xi}{S}\frac{dS}{dt}\frac{\partial u}{\partial \xi}+v\right)+S\frac{\partial\left(\frac{\tau_0 n\rho}{1+\lambda n^2}\right)}{\partial \xi}=0 \tag{A10}$$

The position of the moving sphere boundary in these expressions is defined as $S(t)=1+u_b(t)$, where $u_b(t)$ is the displacement at the sphere boundary (that is, $u(\xi=1, t)$). Using the definition of velocity, $v(\xi, t)$, stated above, then, $v=dS/dt$ at $\xi=1$. The initial conditions Eqs. 11a–11c can be rewritten as:

$$n(\xi, t_0)=n_0 \tag{A11a}$$

$$\rho(\xi, t_0)=1 \tag{A11b}$$

$$u(\xi, t_0)=0 \tag{A11c}$$

and the initial condition for v, obtained from the mechanical force balance at time zero, is:

$$v(\xi, t_0)=\frac{dS}{dt}\xi \tag{A11d}$$

The transformed boundary conditions are:

$$\frac{\partial \rho}{\partial \xi}=0, \quad \xi=0 \tag{A12}$$

$$\frac{\partial n}{\partial \xi}=0, \quad \xi=0 \tag{A13a}$$

$$\frac{\partial n}{\partial \xi}=0, \quad \xi=1 \tag{A13b}$$

$$u=0, \quad \xi=0 \tag{A14a}$$

$$\frac{1}{S}\frac{\partial u}{\partial \xi}+\nu_2\frac{2u}{S\xi}+\frac{\mu_1}{S}\frac{\partial}{\partial \xi}\left(-\frac{\xi}{S}\frac{dS}{dt}\frac{\partial u}{\partial \xi}+v\right)+\frac{2\mu_2}{S\xi}\left(-\frac{\xi}{S}\frac{dS}{dt}\frac{\partial u}{\partial \xi}+v\right)+\tau_0\frac{\rho n}{1+\lambda n^2}=0, \quad \xi=1 \tag{A14b}$$

$$v=0, \quad \xi=0 \tag{A15}$$

The zero stress condition at the moving sphere boundary, Eq. A14b, can be evaluated at time zero to yield the initial velocity of the sphere boundary, dS/dt, away from its initial value $S(0)=1$:

$$\frac{dS}{dt}=\frac{-\tau_0 n_0}{(\mu_1+2\mu_2)(1+\lambda n_0^2)}, \quad t=0 \tag{A16}$$

This expression can then be substituted in Eq. A11d to obtain the initial velocity profile. For clarity, $\partial(\cdot)/\partial\xi$ in Eqs. A10 and A14b is not expanded here.

This transformed nonlinear moving boundary value problem was reduced to a differential/algebraic system of equations by applying centered finite difference approximations to all spatial derivatives (that is, the method of lines). The resulting expressions were solved numerically using DASSL, the differential/algebraic system solving code developed by Linda Petzold (Petzold, 1983).

Appendix B

The system of three nonlinear partial differential equations in transformed coordinates (Eqs. A8–A10) is shown here to admit a solution of the form:

$$n(\xi, t)=n(t) \tag{B1}$$

$$\rho(\xi, t)=\rho(t) \tag{B2}$$

$$u(\xi, t)=h(t)\cdot\xi \tag{B3}$$

which satisfies the initial and boundary conditions (with $h(0)=0$), Eqs. A11–A15. This approach was motivated by the numerical results for the full partial differential equation system (Figure 8). If we let

$$\frac{\partial u}{\partial t}=v=\frac{dh}{dt}\cdot\xi \tag{B4}$$

and define $a(t)$ as

$$\frac{dh}{dt}=a(t) \tag{B5}$$

so that $v=a(t)\cdot\xi$, and knowing from Appendix A that $v=dS/dt$ at $\xi=1$, and thus

$$\frac{dS}{dt}=a(t) \tag{B6}$$

then our system of partial differential equations reduces to:

Cell Conservation Equation:

$$\frac{dn}{dt}=\frac{3na}{S}\left(\frac{h}{S}-1\right)+kn(1-n) \tag{B7}$$

Matrix Conservation Equation:

$$\frac{d\rho}{dt}=\frac{3\rho a}{S}\left(\frac{h}{S}-1\right) \tag{B8}$$

with the mechanical force balance being exactly satisfied. Taking the first derivative of the zero stress boundary condition yields:

$$\frac{da}{dt}=\frac{1}{(\mu_1+2\mu_2)(S-h)}\left\{\frac{\tau_0}{1+\lambda n^2}\left[\frac{2\lambda\rho n^2S^2}{1+\lambda n^2}\times\left(\frac{3na}{S}\left(\frac{h}{S}-1\right)+kn(1-n)\right)-2n\rho a(3h-2S)-kn\rho S^2(1-n)\right]-a(1+2\nu_2)(S+h)\right\} \tag{B9}$$

In this case then, the solution for n, ρ, u, v, and $S(t)$ requires solving only a set of five nonlinear coupled ordinary differential equations for $n(t)$, $\rho(t)$, $h(t)$, $a(t)$, and $S(t)$.

Manuscript received Apr. 23, 1992, and revision received Aug. 3, 1992.